Molecular Biology of the Cell
Vol. 17, 4962–4971, December 2006

Global Organization and Function of Mammalian Cytosolic Proteasome Pools: Implications for PA28 and 19S Regulatory Complexes

Toru Shibatani,* Eric J. Carlson,* Fredrick Larabee,* Ashley L. McCormack,† Klaus Früh,† and William R. Skach*

*Department of Biochemistry and Molecular Biology, Oregon Health & Sciences University, Portland, OR 97201; and †Vaccine and Gene Therapy Institute, Oregon Health & Sciences University, Beaverton, OR 97006-3448

Submitted April 17, 2006; Revised August 14, 2006; Accepted September 13, 2006
Monitoring Editor: Thomas Sommer

Proteolytic activity of the 20S proteasome is regulated by activators that govern substrate movement into and out of the catalytic chamber. However, the physiological relationship between activators, and hence the relative role of different proteasome species, remains poorly understood. To address this problem, we characterized the total pool of cytosolic proteasomes in intact and functional form using a single-step method that bypasses the need for antibodies, proteasome modification, or column purification. Two-dimensional Blue Native(BN)/SDS-PAGE and tandem mass spectrometry simultaneously identified six native proteasome populations in untreated cytosol: 20S, singly and doubly PA28-capped, singly 19S-capped, hybrid, and doubly 19S-capped proteasomes. All proteasome species were highly dynamic as evidenced by recruitment and exchange of regulatory caps. In particular, proteasome inhibition with MG132 markedly stimulated PA28 binding to exposed 20S α-subunits and generated doubly PA28-capped and hybrid proteasomes. PA28 recruitment virtually eliminated free 20S particles and was blocked by ATP depletion. Moreover, inhibited proteasomes remained stably associated with distinct cohorts of partially degraded fragments derived from cytosolic and ER substrates. These data establish a versatile platform for analyzing substrate-specific proteasome function and indicate that PA28 and 19S activators cooperatively regulate global protein turnover while functioning at different stages of the degradation cycle.

INTRODUCTION

The 20S proteasome is a cylindrical multicatalytic protease comprised of two stacked inner rings of proteolytically active β-subunits flanked by two outer rings of α-subunits (Lowe *et al.*, 1995; Groll *et al.*, 1997; Voges *et al.*, 1999; Glickman and Ciechanover, 2002; Pickart and Cohen, 2004). In mammalian cells, proteasome activity is controlled by regulatory complexes (caps) that bind to the exposed ends of α-subunits and open the gate into and out of the catalytic chamber (Hoffman *et al.*, 1992; DeMartino and Slaughter, 1999; Voges *et al.*, 1999; Groll *et al.*, 2000; Kloetzel and Ossendorp, 2004; Rechsteiner and Hill, 2005). One such cap, the 19S regulatory complex (PA700/RC), contains a hexameric ring of AAA-ATPases (base) and at least 12 additional subunits (lid) that recognize, unfold, and translocate polyubiquitinated proteins into the axial opening of the 20S core (Tanaka, 1998; Glickman *et al.*, 1999; Strickland *et al.*, 2000; Leggett *et al.*, 2005; Liu *et al.*, 2005). Two 19S RCs bind the 20S particle to form the doubly capped (30.3S) proteasomes (Yoshimura *et al.*, 1993) that are generally believed to be the major species responsible for degrading polyubiquitinated proteins in the cell (Tanaka and Tsurumi, 1997; Voges *et al.*, 1999; Wolf and Hilt, 2004). 19S RC binding to the 20S core particle requires ATP (Orino *et al.*, 1991), and ATP hydrolysis transiently dissociates 20S and 19S particles, possibly to allow release of degradation products (Babbitt *et al.*, 2005). Thus it has been proposed that the degradation cycle involves dynamic interactions between proteasome subcomplexes.

An alternate proteasome cap consists of ring-shaped heptamers formed by the small 28-kDa protein PA28α, β, or γ (REG α, β, or γ). PA28 was identified nearly a decade ago by the groups of DeMartino and Rechsteiner as an ATP-independent activator that stimulates the degradation of small peptides but not intact or polyubiquitinated proteins (Dubiel *et al.*, 1992; Ma *et al.*, 1992). High-resolution crystal structures have demonstrated that the PA28 homolog, PA26, induces a conformational change in the N-termini of 20S α-subunits that opens the entrance of the catalytic chamber (Whitby *et al.*, 2000; Forster *et al.*, 2005). PA28 (PA26) also alters the proteolytic properties of 20S and/or 19S-20S proteasomes by modifying the pattern, but not the overall size of cleaved products (Harris *et al.*, 2001; Li *et al.*, 2001; Cascio *et al.*, 2002; Wang *et al.*, 2003). PA28αβ subunits are particularly abundant in immune tissues and are coordinately regulated by IFNγ together with β1i, β2i, and β5i subunits of the immunoproteasome, ER peptide transporters (TAP1, TAP2), and MHC class I molecules (Früh and Yang, 1999; Rechsteiner *et al.*, 2000; Kloetzel and Ossendorp, 2004). PA28 expression also stimulates formation of "hybrid" proteasomes contain-

This article was published online ahead of print in *MBC in Press* (http://www.molbiolcell.org/cgi/doi/10.1091/mbc.E06–04–0311) on September 20, 2006.

Address correspondence to: William R. Skach (skachw@ohsu.edu).

Abbreviations used: 19S RC, 19S regulatory subunit; ER, endoplasmic reticulum; PA28, proteasome activator, 28 kDa; RRL, rabbit reticulocyte lysate; BN-PAGE, blue native-polyacrylamide gel electrophoresis.

ing both 19S and PA28 caps (Hendil *et al.*, 1998; Tanahashi *et al.*, 2000). Collectively, these and related findings have suggested that PA28 plays a primary role in antigen presentation by generating a distinct set of peptide fragments that preferentially bind MHC class I molecules (Kloetzel, 2004; Rechsteiner and Hill, 2005).

An important and unresolved issue in proteasome biology is how different regulatory caps contribute to proteolytic function in cells. This is in part due to limitations of conventional purification methodologies, e.g., multistep column chromatography, which are prone to loss of activators in high ionic strength buffers (Tanaka *et al.*, 1988; Driscoll and Goldberg, 1990; Udvardy, 1993; Shibatani and Ward, 1995). Information on the function of PA28 and hybrid proteasomes has therefore been largely derived from in vitro reconstitution experiments using purified PA28, 20S and singly capped 19S-20S proteasomes (Kopp *et al.*, 2001; Cascio *et al.*, 2002; Rechsteiner and Hill, 2005). Although, 20S, 26S, and hybrid proteasomes have been isolated by immunoaffinity purification (Hendil *et al.*, 1998; Saeki *et al.*, 2000; Verma *et al.*, 2000) and column chromatograpy under low ionic strength (Tanahashi *et al.*, 2000), such approaches have had limited success in analyzing the in vivo relationship between different proteasome pools.

We now report a single-step purification scheme using Blue Native(BN)-PAGE that enables us for the first time, to characterize dynamic changes in the global complement of native cytosolic proteasomes. BN-PAGE was initially developed to purify and analyze multimeric membrane protein complexes from mitochondria (Schägger and von Jagow, 1991; Schägger *et al.*, 1994) and has subsequently been extended to the endoplasmic reticulum, chloroplast and peroxisome (Caliebe *et al.*, 1997; Wang and Dobberstein, 1999; Reguenga *et al.*, 2001; Shibatani *et al.*, 2005) as well as cytosolic proteins including proteasomes (Camacho-Carvajal *et al.*, 2004). This technique allows intact multimeric protein complexes to be separated by size with a high degree of precision in the first dimension using Coomassie G250 dye as the negative charge carrier. Components from each complex can then be identified by SDS-PAGE in the second dimension. In combination with liquid chromatography/tandem mass spectrometry, (LC-MS/MS), we simultaneously isolated six major proteasome populations from resting cytosol and identified these species as 20S, singly and doubly PA28-capped (PA28-20S and PA28-20S-PA28), singly 19S-capped (26S), hybrid (PA28-20S-19S), and doubly 19S-capped (30.3S) proteasomes. All proteasome species were highly dynamic, as evidenced by rapid exchange of regulatory complexes in response to cytosolic manipulation. Moreover, proteasome inhibition further stimulated PA28 recruitment and rapidly generated doubly PA28-capped and hybrid proteasomes that remained stably associated with specific subsets of degradation intermediates. These data indicate that PA28 and 19S activators cooperate in general protein turnover and function at different stages of the degradation cycle.

MATERIALS AND METHODS

Preparation and Analysis of Proteasome Fractions

Rabbit reticulocytes lysate (RRL) was prepared by hypotonic lysis (1:1 volume with ddH_2O) of reticulocytes and stored at −80°C as described (Carlson *et al.*, 2005). Ribosomes were removed from 25-μl aliquots of RRL by centrifugation (350,000 × *g* for 1 h at 4°C). Ribosome-free RRL was then diluted fivefold in 20 mM Tris-HCl, pH 7.6, 1 mM DTT, 1 mM ATP, and 1 mM $MgCl_2$ and centrifuged at 350,000 × *g* for 2 h at 4°C. The resulting proteasome pellets were resuspended in 30 μl of buffer A (50 mM HEPES-NaOH, pH 7.8, 75 mM NaCl, 7.5 mM $MgOAc_2$, 2.5 mM DTT, and 7.5% [wt/vol] glycerol). Where indicated, ribosome-free RRL was incubated with the following: 1) 1.0 mM ATP, 12 mM creatine phosphate, and 80 μg/ml creatine kinase (Roche, Indianapolis, IN); or 2) 20 U/ml hexokinase (Sigma, St. Louis, MO) and 20 mM 2-deoxyglucose; or 3) 100 μM Z-Leu-Leu-Leu-CHO (MG132; Sigma) in buffer containing 18 mM sucrose, 18 mM KCl, 3 mM DTT, 5 mM $MgCl_2$, 10 mM Tris-HCl, pH7.5, for 0–60 min at 37°C. Proteasomes were then isolated by ultracentrifugation as described above.

BN-PAGE, Native-PAGE, and Two-dimensional BN/SDS-PAGE

BN-PAGE was based on the protocol described by Schägger *et al.* (1994). Crude proteasome pellets were resuspended in buffer A, loaded directly onto BN-PAGE gels (cast as a 5–13% acrylamide gradient [acrylamide:bis-acrylamide = 32:1] in 50 mM BisTris/HCl, pH 7.0, 500 mM ε-aminocaproic acid [EACA], and overlaid by 4% stacking gel in the same buffer). Electrophoresis was carried out at 4°C at 100 V for 17 h (cathode buffer = 50 mM Tricine, 15 mM BisTris-HCl [pH 7.0] and 0.02% Coomassie G250 [Serva Blue G; Serva Electrophoresis GmbH, Heidelberg, Germany], anode buffer = 50 mM Bis-Tris-HCl, pH 7.0) and then at 500 V for 24 h after reducing Coomassie G250 dye concentration to 0.002%. Thyroglobulin (670 kDa) ferritin (440 kDa) and bovine serum albumen (dimer,133 kDa) were used as molecular weight markers. Clear Native-PAGE (Schägger *et al.*, 1994; Wittig and Schägger, 2005) was carried out in the same manner as BN-PAGE except that the EACA concentration in gel was reduced to 50 mM and Coomassie G-250 dye was omitted in cathode buffer. For Coomassie staining, the gel was fixed in 35% (vol/vol) methanol, 10% (vol/vol) acetic acid, washed three times with H_2O, and incubated in 8% ammonium sulfate, 0.816% phosphoric acid, 0.08% Coomassie G-250, and 20% methanol. Two-dimensional (2D) SDS-PAGE was performed by treating BN-PAGE strips with 1% DTT in 62.5 mM Tris-HCl, pH 6.8, 10% (wt/vol) glycerol, 2% SDS for 20 min at 24°C and alkylating with 2.5% iodoacetamide in 62.5 mM Tris-HCl, pH 6.8, 10% glycerol, 2% SDS for 20 min at 24°C. Gel strips were then placed over an SDS-PAGE (12–17% gradient, 4% stacking gel) and run at room temperature. Gels were scanned using a Umax Power Look III transmission scanner (Lexmark, Dallas, TX). Coomassie-stained bands were quantitated using a Li-Cor Odyssey infrared imaging system (700-nm channel) V.1.2 (Lincoln, NE).

Preparation of Samples for Mass Spectrometry

Silver staining was performed according to the modified Blum method, and samples were extracted by tryptic digestion (Blum *et al.*, 1987; Mortz *et al.*, 2001; Shibatani *et al.*, 2005). Gels were fixed in 40% (vol/vol) ethanol and 10% (vol/vol) acetic acid, washed three times with 30% (vol/vol) ethanol for 20 min, and washed once with ddH_2O. The gel was sensitized with 0.02% NaS_2O_3, washed three times with ddH_2O, incubated with 0.1% silver nitrate for 20 min at 4°C, rinsed three times, and developed with 3% Na carbonate and 0.05% formalin. Protein bands were excised from silver-stained gels, dried, destained in 15 mM K ferricyanide and 50 mM NaS_2O_3 at 24°C for 15 min, and washed with 100 mM NH_4HCO_3. Destained gels fragments were dried, rehydrated with 0.01 mg/ml sequence-grade modified porcine trypsin (Promega, Madison, WI) in 50 mM NH_4HCO_3 and 5 mM $CaCl_2$, and incubated at 37°C overnight. Trypsinized fragments were collected by bath sonication in 50 μl of 25 mM NH_4HCO_3 and again after adding 50 μl of 50% acetonitrile. The supernatant was collected, and the gel fragment was sonicated repeatedly in 50 μl of 5% formic acid and again after adding 50 μl of 50% acetonitrile. Supernatants were pooled. DTT was added to a final concentration of 1 mM. The sample was dried and stored at −80°C before analysis.

Mass Spectrometry

Samples were dissolved in 5% formic acid before liquid chromatography using a 10 cm × 180 μm Biobasic-C18 capillary column (Thermo Hypersil Keystone, West Palm Beach, FL) and analysis by electrospray ionization tandem mass spectrometry (MS/MS) using an LCQ Deca XP Plus ion trap mass spectrometer (ThermoElectron, San Jose, CA). Peptides were eluted using a mobile phase of 0.1% formic acid in water and either a 30-min 0–50% acetonitrile gradient or a 110-min 0–45% acetonitrile gradient. The instrument was set to trigger data-dependent MS/MS acquisition of the three most intense ions detected during the MS survey scan. Mass spectra were analyzed with the Sequest algorithm (ThermoElectron) as described by Eng and coworkers (Eng *et al.*, 1994) using the UniProt/Swiss-Prot protein database (Uniprot release 5.1, URL: http://www.us.expasy.org/, Accessed 5/13/05). Search results were further analyzed by PeptideProphet (Keller *et al.*, 2002) and ProteinProphet (Nesvizhskii *et al.*, 2003) (Seattle Proteome Center, URL: http://tools.proteomecenter.org/windows.php). Proteins identified by ProteinProphet utilized a probability cutoff of $p > = 0.99$, which corresponded to an error of 0.002. Peptides were included in the coverage calculation when the adjusted PeptideProphet probability was greater than or equal to 0.9. All results were manually inspected.

Peptidase Assays

RRL proteasomes were preincubated for 30 min on ice in 50 mM BisTris-HCl, pH 7.0, containing 50 or 500 mM EACA or 0.01% of Coomassie G250. Reactions were then incubated for 30 min at 37°C with 100 μM *N*-succinyl-

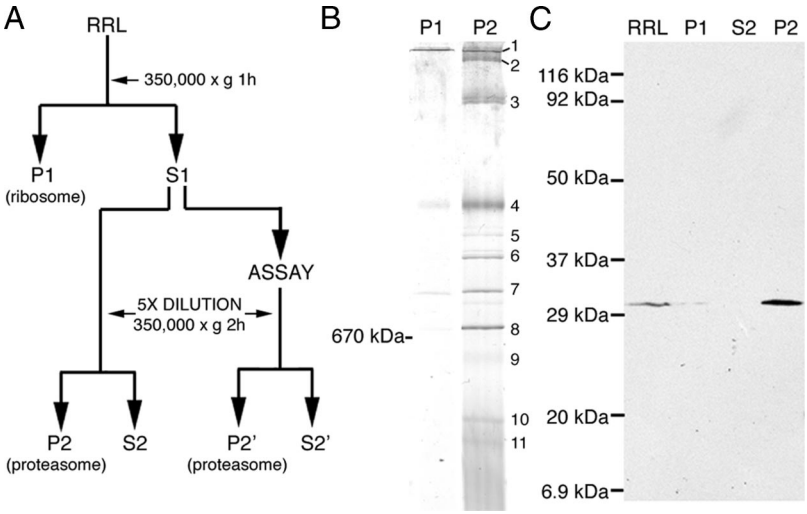

Figure 1. (A) Strategy for isolation of RRL proteasomes by differential centrifugation. (B) The initial ribosome pellet (P1) and proteasome pellet (P2) were separated by BN-PAGE and stained with Coomassie G-250. A single major species predominated in P1 fraction, and 11 major bands were visualized in P2, several of which appeared as closely spaced doublets. (C) RRL, P1, S2, and P2 fractions were analyzed by SDS-PAGE and Western blotting using antisera raised against the 20S α3-subunit.

Leu-Leu-Val-Tyr-7-amido-4-methylcoumarin (sLLVY-AMC) in buffer B (50 mM Tris-HCl, pH 7.5, 5 mM $MgCl_2$, 10 mM KCl, 1 mM DTT, 1 mM ATP) in the presence of 50 or 500 mM EACA or 0.0012% Coomassie G250. The reaction was stopped by adding 2 volumes of 100% ethanol, and AMC fluorescence was measured at 380 nm/440 nm excitation/emission (Hoffman *et al.*, 1992; Oberdorf *et al.*, 2001). For in-gel assays, BN- and CN-PAGE gel strips were incubated at 37°C for 30 min with 200 μM sLLVY-AMC in buffer B. The gel was exposed and photographed using a UV transiluminator (Gel Doc 1000, Bio-Rad, Hercules, CA).

Western Blotting

Proteins were transferred to PVDF membranes, blocked with 5% dried milk, incubated with rabbit PA28β antisera (1:2000 dilution) raised against peptides encoding C-terminal 21 amino acid residues of PA28β (Ahn *et al.*, 1996) or anti-proteasome antisera raised against the recombinant murine α-3 20S subunit (Yang *et al.*, 1995). Signals were obtained using horseradish peroxidase–conjugated goat anti-rabbit secondary antibody (1:5000 dilution; Bio-Rad) using SuperSignal (Pierce, Rockford, IL) according to the manufacturer's instructions.

Protein Degradation and Release Assay

Cystic fibrosis transmembrane conductance regulator (CFTR) was translated in vitro in RRL supplemented with [^{35}S]Met and canine pancreas rough microsomal membranes (Carlson *et al.*, 2005). Microsomes containing integrated CFTR were isolated by pelleting (180,000 × *g* for 10 min) through 0.5 M sucrose in buffer C (100 mM KoAc, 5 mM $Mg(OAc)_2$, 1 mM DTT, and 50 mM HEPES-

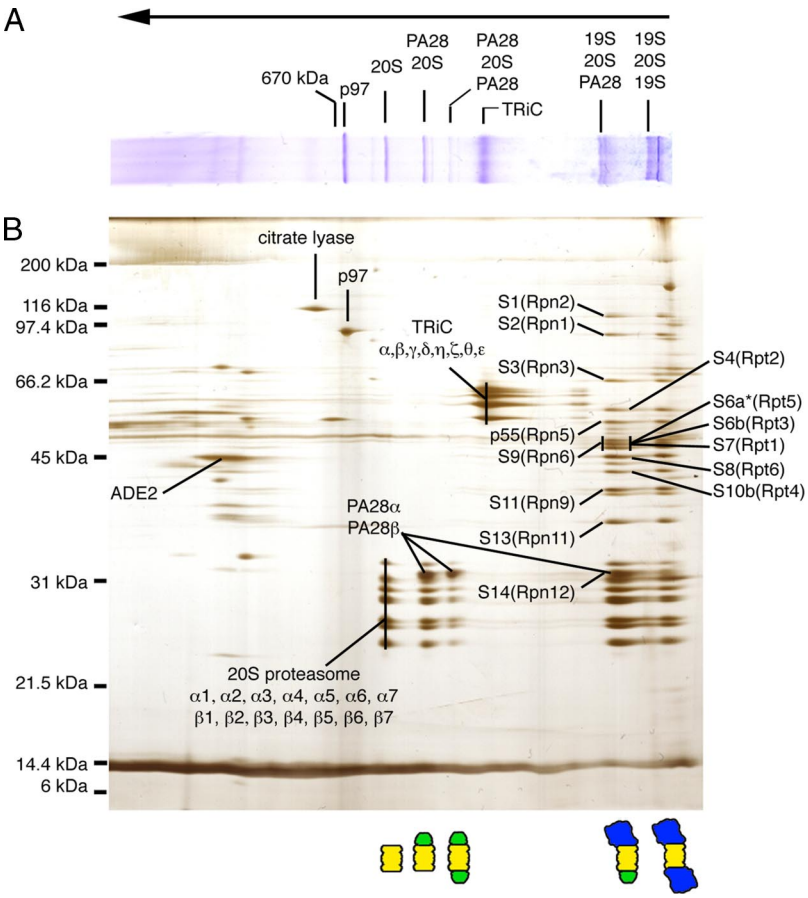

Figure 2. (A) BN-PAGE gel from proteasome fraction (P2) was subjected to SDS-PAGE in the second (vertical) dimension. (B) Silver-stained 2D-BN/SDS-PAGE gel. Bands of interest were excised, trypsin-digested, and subjected to analysis by LC-MS/MS. Identities and corresponding locations of proteins are indicated. 19S RC subunits are based on nomenclature of human erythrocyte proteasomes (Dubiel *et al.*, 1995) with corresponding yeast subunits (*Saccharomyces cerevisiae*) shown in parentheses (Finley *et al.*, 1998). Identity and location of capped proteasome populations is diagrammed at the bottom. 20S proteasome is shown in yellow, PA28 in green, and 19S RC in blue. Migration of thyroglobulin marker (670 kDa) in BN-PAGE is indicated on the top.

Table 1. Major proteins identified in this analysis

Complex	Subunits	Accession number		MW	Peptides ID	Sequence coverage (% amino acids)
		Swissprot	NCBI			
20S	α1	PSA6_HUMAN	46397659	27399	10	42.3
	α2	PSA2_HUMAN	130850	25767	5	21.5
	α3	PSA4_HUMAN	130861	29484	6	21.8
	α4	PSA7_HUMAN	12643540	27887	8	24.6
	α5	PSA5_HUMAN	38258905	26411	6	34.4
	α6	PSA1_HUMAN	130848	29556	9	35.4
	α7	PSA3_HUMAN	130859	28302	8	27.6
	β1	PSB6_HUMAN	20532407	25358	3	13.0
	β2	PSB7_HUMAN	17380263	29965	5	17.3
	β3	PSB3_HUMAN	20532411	22949	8	40.0
	β4	PSB2_HUMAN	1709762	22836	6	31.3
	β5	PSB5_HUMAN	1172607	22897	8	36.5
	β6	PSB1_HUMAN	130853	26489	5	24.5
	β7	PSB4_HUMAN	3915810	29192	2	13.3
PA28	α	PSME1_HUMAN	1170519	28723	3	14.5
	β	PSME2_HUMAN	18203506	27230	3	12.6
19S	S1 (Rpn2)	PSD1_HUMAN	51704332	105836	3	3.9
	S2 (Rpn1)	PSD2_HUMAN	6174930	100200	4	5.0
	S3 (Rpn3)	PSD3_HUMAN	20532405	60978	16	26.4
	p55 (Rpn5)	PSD12_HUMAN	20978544	52904	4	8.3
	S4 (Rpt2)	PRS4_HUMAN	49065817	49185	3	7.0
	S6a (Rpt5)	PRS6A_HUMAN	20532406	49204	1[a]	2.1
	S6b (Rpt3)	PRS6B_HUMAN	20532409	47366	4	11.7
	S7 (Rpt1)	PRS7_HUMAN	547930	48503	8	21.5
	S8 (Rpt6)	PRS8_HUMAN	49065819	45626	7	19.0
	S9 (Rpn6)	PSD11_HUMAN	20978543	47333	12	32.8
	S10a (Rpt4)	PRS10_HUMAN	51702772	44173	5	14.1
	S11 (Rpn9)	PSD13_HUMAN	20978558	42918	7	17.8
	S13 (Rpn11)	PSDE_HUMAN	51701716	34577	2	6.5
	S14 (Rpn12)	PSD8_HUMAN	1346766	30005	2	7.0
p97		TERA_HUMAN	6094447	89191	20	30.3
TRiC	α	TCPA_HUMAN	135538	60344	11	21.9
	β	TCPB_HUMAN	6094436	57357	13	28.3
	γ	TCPG_HUMAN	66774185	60534	18	33.9
	δ	TCPD_HUMAN	52001478	57793	7	16.2
	η	TCPH_HUMAN	3041738	59367	18	39.0
	ζ	TCPZ_HUMAN	730922	57893	7	19.2
	θ	TCPQ_HUMAN	9988062	59489	18	35.8
	ϵ	TCPE_HUMAN	1351211	59671	11	20.3
Citrate lyase		ACLY_HUMAN	20141248	120825	16	18.3
ADE2		PUR6_HUMAN	131628	46948	9	25.2

[a] Only one peptide fragment was identified.

NaOH, pH 7.5) and resuspended in buffer C containing 0.1 M sucrose. In vitro degradation conditions were exactly as described elsewhere (Carlson *et al.*, 2005). Samples were incubated for 2 h at 37°C in the presence of 100 μM MG132. Cytosolic CFTR fragments released during the reaction were recovered by pelleting membranes through 0.5 M sucrose in buffer C (180,000 × *g* for 10 min). Proteasomes in the supernatant were subsequently isolated by ultracentrifugation as above and separated by 2D BN-PAGE/SDS-PAGE. Gels were fixed, silver-stained, dried, and exposed to Kodak film (Eastman Kodak, Rochester, NY). ^{14}C-methylated lysozyme (Sigma) was incubated in the identical RRL degradation system. Proteasomes were separated by BN-PAGE, and the gel was stained with silver or Coomassie G-250 and imaged by autoradiograpy.

RESULTS

Cytosolic proteasomes were collected from RRL by differential sedimentation (Figure 1A), and crude pellets were resuspended and analyzed directly by BN-PAGE (Figure 1B) or SDS-PAGE (Figure 1C). Eleven distinct protein bands (>440 kDa in size) were readily detected by Coomassie staining (Figure 1B). Immunoblotting for the 20S α3-subunit (Figure 1C) and quantitation of Coomassie stained gels revealed that this process recovered ~90% of total RRL proteasomes for analysis. BN-PAGE gel strips were subsequently analyzed in the second dimension by SDS-PAGE (Figure 2B), and silver-stained bands were then excised and subjected to tryptic digestion, liquid chromatography, and tandem mass spectrometry (LC-MS/MS). Uninterpreted MS/MS spectra were analyzed using the Sequest algorithm, and results were filtered using PeptideProphet and ProteinProphet as described in *Materials and Methods*. Major proteins identified in this analysis included all 14 α and β subunits of the 20S proteasome, PA28α and PA28β, 14 subunits of the 19S RC, all 8 subunits of the cytosolic chaperonin TRiC and p97(VCP/cdc48; Figure 2B and Table 1).

Based on the signature pattern of the 20S core subunits, 5 of the 11 protein complexes visualized by BN-PAGE were unequivocally identified as proteasomes. The smallest species was comprised exclusively of 20S α- and β-subunits and

thus represented free 20S particles (~750 kDa). Two slightly larger species contained an additional pair of proteins identified as PA28α and PA28β. The size of these complexes and the relative intensity of PA28 staining indicate that they represent singly and doubly PA28-capped proteasomes, respectively (~900 and ~1100 kDa). The two largest proteasome species contained 20S particles and at least 14 known subunits of the 19S RC. One of these contained 19S RC and PA28$\alpha\beta$ and therefore represents hybrid (PA28-20S-19S) proteasomes. This complex migrated as a closely spaced doublet and also contained singly 19S-capped (19S-20S) proteasomes (see also Figure 4B). In contrast, the largest complex lacked PA28 and contained 19S and 20S subunits and constitutes doubly 19S-capped (19S-20S-19S) proteasomes. Thus, in a single-step purification, we show that unstimulated cytosol contains substantial amounts of 20S, PA28-20S, 19S-20S, PA28-20S-19S, and 19S-20S-19S proteasomes and relatively small amounts of PA28-20S-PA28 proteasomes.

Purified Proteasomes Retain Peptidase Activity

To determine whether isolated proteasomes retained function, in-gel assays were performed using the fluorogenic peptide substrate sLLVY-AMC. Initial experiments using BN-PAGE gels failed to reveal peptidase activity (Figure 3A, lanes 1 and 2), suggesting that components in the gel might inhibit proteasomes. Consistent with this, we showed that Coomassie G-250 was a potent inhibitor of chymotrypsin-like activity (>90% inhibition), whereas a high concentrations of ε-aminocaproic acid (500 mM) produced a mild reduction (50%) in substrate cleavage (Figure 3B). RRL was therefore subjected to a variation of BN-PAGE (previously termed Clear-Native PAGE; Schägger *et al.*, 1994; Wittig and Schägger, 2005) using similar gel conditions conditions but omitting Coomassie G-250 dye in the cathode buffer and reducing the EACA concentration to 50 mM. As previously reported (Wittig and Schägger, 2005), native-PAGE resulted in less resolution and a more complex staining pattern than BN-PAGE (Figure 3C). However, five distinct 20S proteasome complexes were identified, and in-gel assays demonstrated that four of these retained peptidase activity. These active complexes also comigrated with PA28-capped and 19S-capped proteasomes (Figure 3, A, lane 3, and C). Given the reduced resolution of native-PAGE, however, we could not conclusively determine whether hybrid and singly 19S-capped proteasomes were both present in the second largest band. As expected, isolated 20S particles lacked proteolytic activity due to the native closed conformation of α-subunit N-termini (Groll *et al.*, 2000). Several heterogeneous bands containing 19S RC subunits were also visualized by native PAGE. This confirmed the presence of 19S RC in RRL, which was likely partially dissociated during electrophoresis due to the increased lability of free particles. Intact 19S RC was not visualized by BN-PAGE, suggesting that it is also sensitive to the harsher gel conditions.

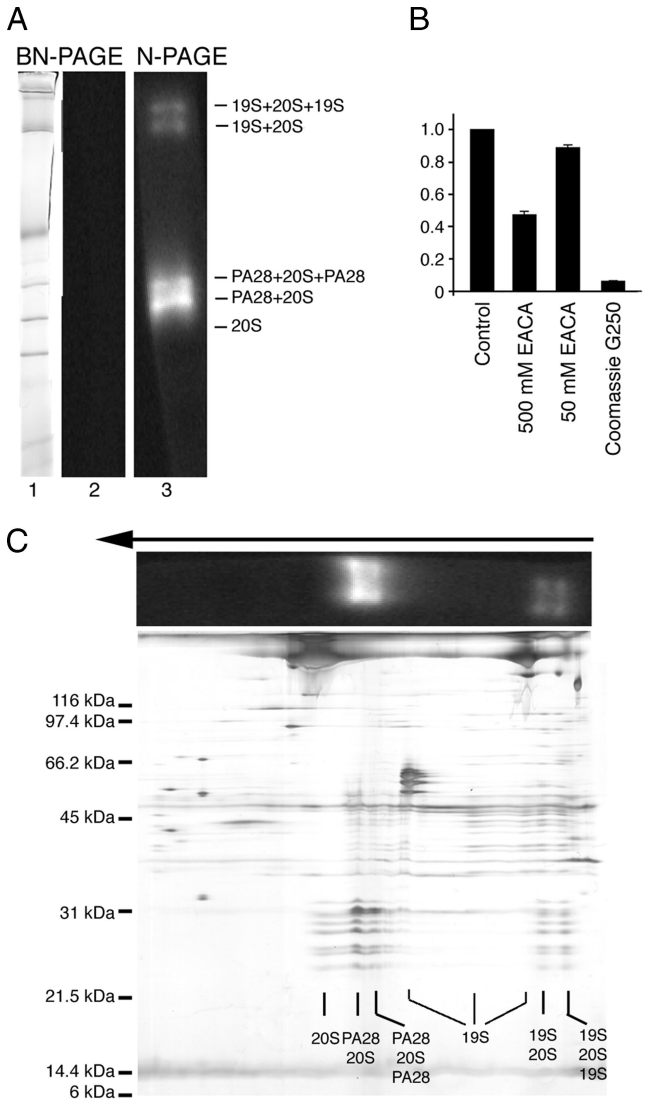

Figure 3. (A) RRL proteasomes were separated by BN-PAGE or CN-PAGE. Gel strips were incubated with sLLVY-AMC and Coomassie stained (lane 1) or photographed using a UV transilluminator Gel-doc (Bio-Rad; lanes 2 and 3). (B) Peptidase activity of RRL proteasomes was determined using sLLVY-AMC in the presence of 0 mM (control), 50 mM, and 500 mM EACA or 0.01% Coomassie G-250. Values were normalized to control conditions. (C) Proteasomes separated by CN-PAGE (A) were subsequently separated by SDS-PAGE to verify the location and composition of active proteasomes.

Proteasome Inhibition Stimulates PA28 Binding to 20S Particles

We next investigated whether RRL proteasomes represented static or dynamic populations. Incubation at 37°C in the presence of ATP substantially increased the fraction of 19S capped proteasomes and correspondingly decreased free 20S particles (Figure 4A, lanes 1–3). In contrast, ATP depletion caused rapid dissociation of 19S-capped complexes as predicted (Orino *et al.*, 1991) and resulted in a slight increase in singly PA28-capped proteasomes, presumably due to release of 19S RC from hybrid proteasomes (Figure 4A, lanes 4–6). Surprisingly, β-subunit inhibition also had a dramatic effect on the proteasome profile. MG132, a potent inhibitor that blocks all three catalytic β-subunit activities (Rock *et al.*, 1994; Bogyo *et al.*, 1997; Oberdorf *et al.*, 2001), markedly stimulated PA28 recruitment and rapidly converted nearly all 20S proteasomes to doubly PA28-capped proteasomes (Figure 4, A, lanes 7–9, and B). Although a mild increase in 19S binding was observed for some experiments, this effect was not reproducible. MG132 also stimulated the formation of hybrid proteasomes as demonstrated by a slight increase in size of the 19S-20S proteasome complex (Figure 4B) and PA28 immunoblotting (Figure 4C). Within minutes of adding inhibitor, PA28 was bound to essentially all free ends of exposed α-subunits (Figure 4, C and D). When MG132 was

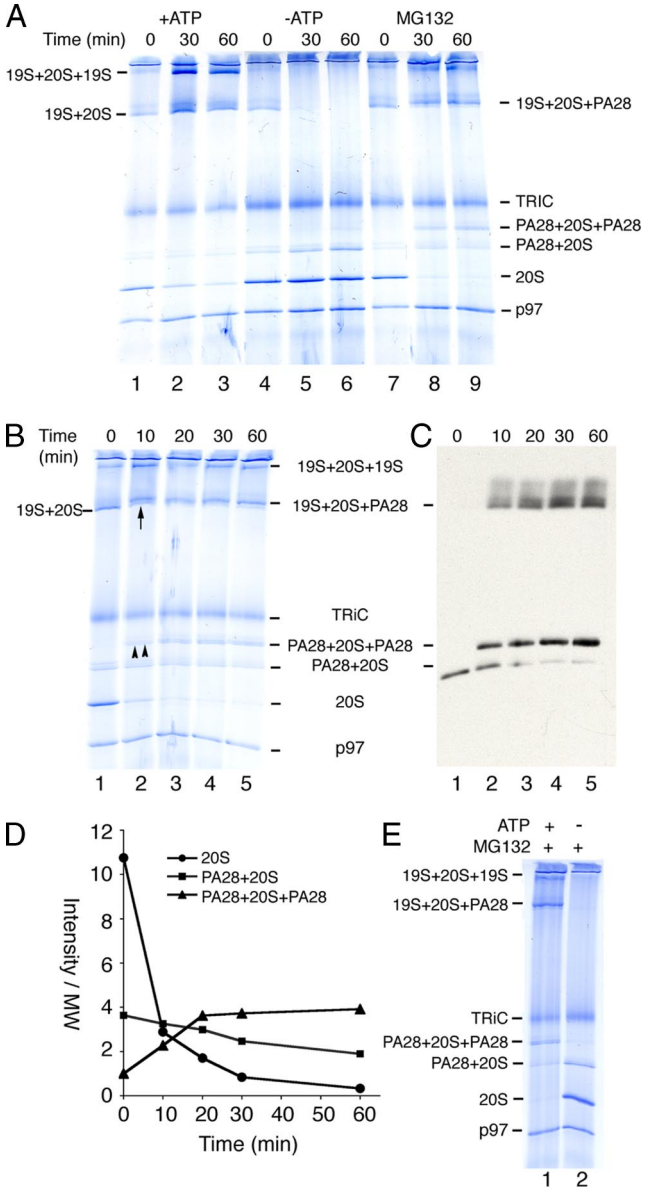

Figure 4. (A) Ribosome-free RRL was incubated at 37°C under the conditions indicated and proteasomes were pelleted, separated by BN-PAGE, and subjected to Coomassie staining. Migration of proteasomes and TRiC is indicated on right. (B and C) Time course of RRL incubation in 100 μM MG132. (B) Coomassie staining and (C) immunoblotting for PA28 revealed rapid formation of doubly capped PA28 and hybrid proteasomes (double and single upward arrows, respectively; lane 2). (D) Quantitation of Coomassie-stained gels showing time course of PA28 recruitment and corresponding decrease in free 20S and singly capped PA28 proteasomes. (E) ATP supplemented (lane 1) or ATP depleted (lane 2) RRL was incubated for 1 h with MG132, and proteasomes were then pelleted and analyzed as in A.

added after ATP depletion, however, 19S caps were released but no additional doubly capped PA28 or hybrid proteasomes were formed (Figure 4E). Thus, even though PA28 does not require ATP to bind the 20S core in vitro and addition of cytosolic ATP by itself did not appreciably stimulate PA28 association (Figure 4A), PA28 recruitment in cytosol is controlled by ATP-dependent mechanisms (discussed further below).

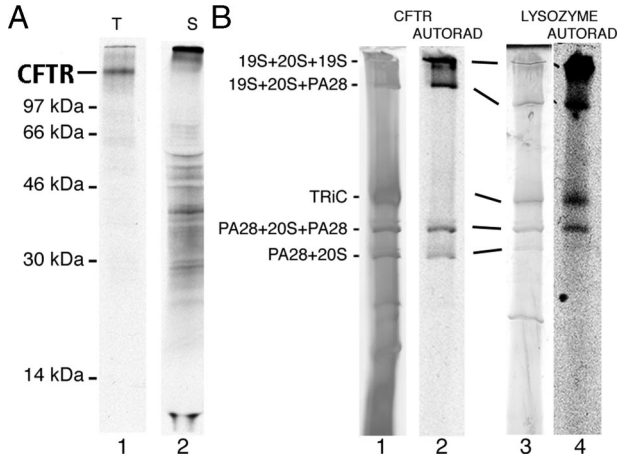

Figure 5. (A) Autoradiogram of SDS-PAGE gel showing translation products (t) for in vitro–translated CFTR (lane 1) and cytosolic degradation intermediates released into the supernatant (s) in the presence of MG132 (lane 2). Input for lane 2 is six times that of lane 1 to better visualize the heterogeneous distribution of degradation products. (B) BN-PAGE analysis of cytosolic fragments of [^{35}S]-CFTR (lanes 1 and 2) and ^{14}C-lysozyme (lanes 3 and 4) after degradation in RRL in the presence of MG132. Migration of proteasomes was determined by silver or Coomassie staining (lanes 1 and 3, respectively), and gels were then subjected to autoradiography (lanes 2 and 4). Migration of hybrid proteasomes varied somewhat because of gel conditions. CFTR fragments comigrated precisely with four distinct proteasome species (lane 2), whereas lysozyme was bound to both proteasomes and the TRiC complex (lane 4).

19S and PA28 Caps Cooperate in Degrading Soluble and Membrane-bound Substrates

The hallmark of proteasome-mediated degradation is ATP-dependent conversion of substrate into small, trichloroacetic acid (TCA)-soluble peptides ~8–20 aa in length. However, we previously showed that when proteolytic β-subunits are severely compromised (e.g., by MG132), substrates continue to be unfolded, and large degradation intermediates accumulate and remain bound to proteasomes (Oberdorf *et al.*, 2006). These findings prompted us to investigate which population(s) of proteasomes participate in the degradation (and sequestration) of specific substrates. Two well-defined substrates were examined, the polytopic membrane protein CFTR and the soluble protein lysozyme, both of which are efficiently degraded into TCA soluble fragments by the RRL ubiquitin-proteasome pathway (Hershko *et al.*, 1984; Xiong *et al.*, 1999; Oberdorf *et al.*, 2001).

To identify proteasome species involved in degradation, we used an in vitro system previously developed in our laboratory that reconstitutes biosynthesis and ER-associated degradation (ERAD) of misfolded integral membrane proteins (Xiong *et al.*, 1999; Oberdorf *et al.*, 2001; Carlson *et al.*, 2005). In this system, in vitro–translated CFTR generates full length (~160 kDa) ^{35}S-labeled protein that is cotranslationally glycosylated and integrated into ER microsomal membranes (Figure 5A, lane 1, and Xiong *et al.*, 1999). When microsomes were isolated and incubated in RRL in the presence of MG132, large heterogeneous CFTR-derived fragments were released from the membrane and accumulated in the cytosol (Figure 5A, lane 2). Previous analyses has shown that these cytosolic fragments originate from membrane-bound, newly synthesized CFTR as a result of ATP-dependent retrotranslocation (Carlson *et al.*, 2006; Oberdorf *et al.*, 2006). When analyzed by BN-PAGE, cytosolic CFTR degradation intermediates specifically comigrated with four

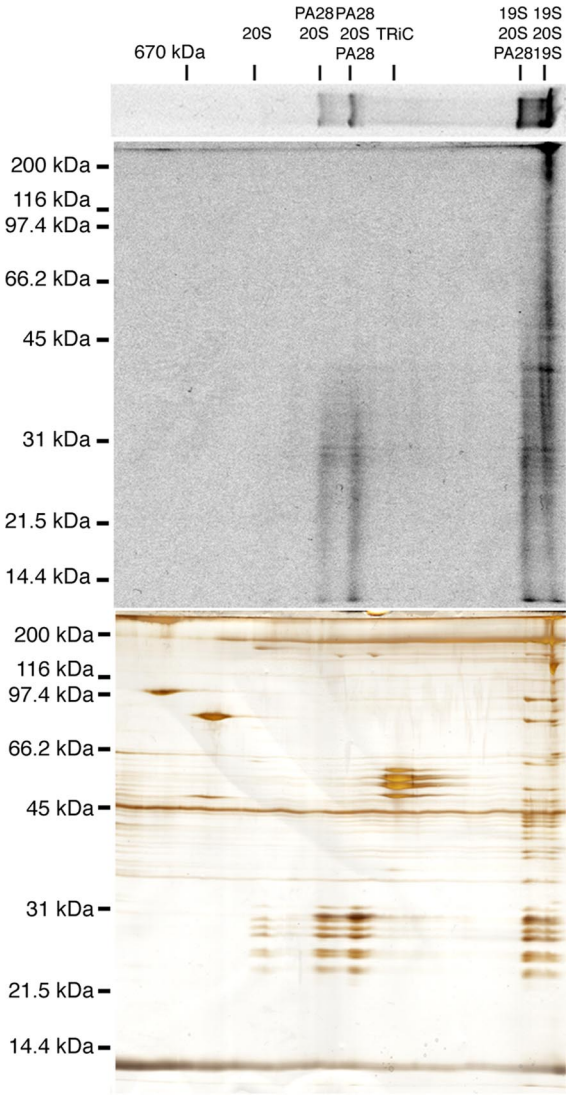

Figure 6. BN-PAGE gel strip from Figure 5 containing cytosolic CFTR fragments was separated by 2D SDS-PAGE and analyzed by autoradiography (top) and silver staining (bottom).

distinct complexes that were identified as singly and doubly PA28-capped, hybrid, and doubly 19S-capped proteasomes (Figure 5B). Similarly, ^{14}C lysozyme was also recovered together with PA28-capped, hybrid, and 19S-capped proteasomes in the presence of MG132 (Figure 5B, lanes 3 and 4). Thus sequestration of degradation intermediates by inhibited, capped proteasomes is a general process that is not restricted to ERAD substrates. Interestingly, lysozyme was also recovered with the cytosolic TRiC complex. This suggests that a subset of lysozyme molecules may also be involved in refolding and that both proteasomes and TRiC maintain their native structure and substrate-binding properties during BN-PAGE purification.

19S and PA28 Capped Proteasomes Bind Different Cohorts of Degradation Intermediates

Finally, we tested whether different proteasome species sequester different distributions of degradation products by comparing autoradiograms and silver-stained 2D BN/SDS-PAGE gels (Figure 6). These results confirmed that CFTR fragments comigrated precisely with specific proteasome species. Doubly 19S-capped proteasomes remained bound to the entire range of CFTR degradation products including fragments larger than CFTR (>160 kDa), which presumably contain polyubiquitin chains that have not yet been removed. In contrast, singly and doubly PA28-capped proteasomes bound primarily to smaller fragments less than ~40 kDa, whereas hybrid proteasomes contained small and intermediate sized fragments (<40 to ~60 kDa). Thus each capped proteasome subtype sequestered a distinct but overlapping subpopulation of degradation intermediates that were derived from a single full-length substrate. Interestingly, no CFTR fragments were recovered with the chaperonin complex TRiC or with p97, an AAA-ATPase that specifically stimulates CFTR degradation by facilitating extraction of its transmembrane domains (Gnann *et al.*, 2004; Carlson *et al.*, 2006; Oberdorf *et al.*, 2006). Thus although p97 likely interacts with CFTR as degradation is initiated, it appears to be released after the substrate is transferred to the proteasome.

DISCUSSION

This study describes the first simultaneous isolation and characterization of total mammalian cytosolic proteasome pools in an intact, native and functional form. 2D BN/SDS-PAGE provides a relatively simple, high-resolution method for single-step isolation that bypasses the need for multiple column chromatography, proteasome antibodies, or proteasome subunit modification. Together with LC-MS/MS, this approach unambiguously identified six different proteasome species as 20S, singly and doubly PA28-capped, singly 19S-capped, hybrid, and doubly 19S-capped proteasomes. With the exception of doubly PA28-capped proteasomes, which were present in relatively low quantities, substantial amounts all other proteasome species were readily identified in freshly thawed, untreated RRL (Figure 2). Native-PAGE confirmed proteolytic activity in at least four proteasome species. Although native-PAGE has been widely used to study the composition, assembly, and functional characteristics of purified 20S and 19S RC particles (Leggett *et al.*, 2002, 2005; Elsasser *et al.*, 2005), the improved resolution of BN-PAGE now allows similar analyses to be performed directly from crude cellular lysates (Camacho-Carvajal *et al.*, 2004). This enabled us to demonstrate that cellular proteasomes are remarkably dynamic and undergo rapid exchange and/or redistribution of regulatory caps in response to changes in the cellular environment. Interestingly, PA28-capped proteasomes constitute a significant fraction of the proteasome pool and appear to participate in degrading diverse substrates. These studies thus establish a powerful tool to monitor the physiological composition and organization of the global proteasome pool and to investigate how different regulatory caps carry out proteolytic activities in cells.

Although the existence of differentially capped proteasomes was established more than a decade ago (Hoffman *et al.*, 1992), little is known regarding the in vivo relationships between different proteasome species, in part because of technical difficulties in isolation and the lability of native complexes (Tanaka *et al.*, 1988; Driscoll and Goldberg, 1990; Udvardy, 1993; Shibatani and Ward, 1995; Hendil *et al.*, 1998; Tanahashi *et al.*, 2000). BN-PAGE now overcomes this constraint by allowing isolation of proteasomes under mild conditions that have little apparent effect on rearrangement or loss of bound caps. Consistent with this, modulation of ATP levels before BN-PAGE recapitulated the known ATP-

dependence of 19S RC binding and yielded predictable changes in the fraction of 26S and 20S proteasomes. Similarly, the pool of free 20S particles was almost completely converted into PA28 capped proteasomes upon incubation with MG132. The rapid recruitment and exchange of 19S RC and PA28 complexes suggests that cytosolic proteasome populations reflects a steady state distribution governed by the relative rates of cap binding and release, which in turn is likely controlled by the specific needs of the cell.

A particularly striking finding was that virtually all exposed ends of 20S subunits were capped by PA28 within minutes of MG132 treatment. Although the exact mechanism of PA28 recruitment is not yet established, several possibilities can be envisioned. MG132 binding to β1-, β2-, and/or β5-subunits in the 20S cylinder could induce an allosteric conformational change that increases the affinity of free α-subunit ends for the PA28 heptamer. This would be consistent with a functional connection between 20S α- and β-subunits as suggested by the ability of PA28 to modulate β-subunit cleavage specificity (Li *et al.*, 2001; Cascio *et al.*, 2002). Alternatively, MG132 could exert indirect effects on RRL that might lead to PA28 association.

A third and intriguing possibility is that PA28 binding might be stimulated by the presence of substrate within the catalytic 20S core. PA28 is proposed to bind the free end of 19S-20S proteasomes where it induces a conformational change in α-subunits that gates open the chamber and facilitates the release of small peptide fragments (Whitby *et al.*, 2000; Forster *et al.*, 2005). However, when cleavage is prevented by MG132, partially degraded fragments derived from both soluble and transmembrane substrates remained bound to PA28-capped proteasomes (Figure 5 and Oberdorf *et al.*, 2006). Importantly, PA 28 recruitment was not significantly affected by ATP levels but was completely abolished when 19S caps were released by ATP depletion before MG132 addition. These findings are consistent with previous reports that ATP stimulates formation of PA28-capped proteasomes in Hela cell extracts (Tanahashi *et al.*, 2000). Moreover, they suggest that substrate translocation (and/or accumulation), rather than MG132 binding, might allosterically increase the affinity of exposed α-subunit N-termini for PA28. If this were the case, then PA28 could be mechanistically coupled to the proteolytic cycle, binding 20S as fragments accumulate and releasing as the core is emptied. Trapped substrates might also maintain the free 20S end in a relatively open conformation, thus favoring PA28 binding. Although speculative, such a model would explain why relatively few doubly capped PA28 proteasomes are present in resting RRL and why it has been difficult to isolate native PA28-20S complexes from cells where functional proteasomes generate small peptide fragments that are readily released (Tanahashi *et al.*, 2000; Cascio *et al.*, 2002).

Our results also revealed that inhibited proteasome species trap fragments of different lengths. Because all of these fragments were derived from a single substrate (CFTR), they likely represent different stages of the degradation cycle. Doubly 19S-capped proteasomes remained associated with the entire range of cytosolic CFTR fragments, consistent with their ability to recognize ubiquitinated substrates and degrade intact proteins and small peptides. In contrast, PA28-capped proteasomes primarily contained peptides less than ~40 kDa in size, and hybrid proteasomes contained only slightly larger fragments. Although it is difficult to precisely extrapolate from inhibited to fully functional proteasomes, these results suggest that doubly 19S-capped proteasomes initiate degradation of intact ubiquitinated substrates and then recruit PA28 as degradation proceeds, perhaps as a consequence of ATP-dependent 19S RC dissociation (Babbitt *et al.*, 2005). Such a process could initially form hybrid proteasomes and lastly PA28-capped proteasomes that complete degradation of deubiquitinated smaller polypeptides (Ma *et al.*, 1992). Alternatively, our results do not rule out the possibility that substrates and/or degradation intermediates could be transferred to different proteasome subtypes as they are de-ubiquitinated and progressively cleaved. In either case the relative distribution of proteasome species would likely reflect total complement of ongoing degradation cycles in the cell at any given time.

Finally, a significant body of evidence has implicated hybrid proteasomes in MHC class I antigen presentation (Hendil *et al.*, 1998; Tanahashi *et al.*, 2000; Cascio *et al.*, 2002), wherein PA28$\alpha\beta$ is proposed to modulate peptide cleavage and preferentially generate antigenic peptides (Hendil *et al.*, 1998; Cascio *et al.*, 2002). Reticulocytes lack intracellular organelles and thus do not present MHC-restricted antigens (Hoffman *et al.*, 1992). It seems likely therefore that reticulocyte PA28 is primarily involved in protein degradation during the various stages of erythrocyte maturation (Etlinger and Goldberg, 1977; Wefes *et al.*, 1995). It is unknown whether PA28 might produce a specific subset of peptides needed for erythrocyte differentiation. However, the high levels of PA28 relative to 20S, the robust induction of hybrid proteasomes after MG132 treatment, and their relative promiscuity in binding to diverse substrates suggests that PA28 likely plays a general role in protein turnover. On the other hand, the distribution of proteasomes observed here may also reflect specialized features of the highly active ubiquitin–proteasome system utilized by reticulocytes during final stages of degrading unneeded residual proteins. Although further investigations are clearly required to delineate the precise role of different proteasome species in different cell types and under different growth conditions, our data demonstrate that multiple proteasomes can participate in the degradation of a single substrate and provide a new approach for investigating physiological relationships between proteasome populations.

ACKNOWLEDGMENTS

The authors thank Dr. L. Musil and members of the Skach lab for valuable advice and comments. This work was supported National Institutes of Health Grants GM53457 (W.S.), DK51818 (W.S.), and T32HL07781 (T.S.) and Core Grant EY10572 (K.F.) and by the Cystic Fibrosis Foundation Therapeutics (W.S.).

REFERENCES

Ahn, K., Erlander, M., Leturcq, D., Peterson, P. A., Früh, K., and Yang, Y. (1996). In vivo characterization of the proteasome regulator P.A28. J. Biol. Chem. *271*, 18237–18242.

Babbitt, S. E., *et al.* (2005). ATP hydrolysis-dependent disassembly of the 26S proteasome is part of the catalytic cycle. Cell *121*, 553–565.

Blum, H., Beier, H., and Gross, H. J. (1987). Improved silver staining of plant proteins, RNA, and DNA in polyacrylamide gels. Electropheresis *8*, 93–99.

Bogyo, M., McMaster, J. S., Gaczynska, M., Tortorella, D., Goldberg, A. L., and Ploegh, H. (1997). Covalent modification of the active site threonine of proteasomal beta subunits and the *Escherichia coli* homolog HslV by a new class of inhibitors. Proc. Natl. Acad. Sci. USA *94*, 6629–6634.

Caliebe, A., Grimm, R., Kaiser, G., Lubeck, J., Soll, J., and Heins, L. (1997). The chloroplastic protein import machinery contains a Rieske-type iron-sulfur cluster and a mononuclear iron-binding protein. EMBO J. *16*, 7342–7350.

Camacho-Carvajal, M., Wollscheid, B., Aebersold, R., Steimle, V., and Schamel, W. (2004). Two dimensional Blue Native/SDS gel electrophoresis of multi-protein complexes from whole cellular lysates. Mol. Cell. Proteomics *3*, 176–182.

Carlson, E., Bays, N., David, L., and Skach, W. R. (2005). Reticulocyte lysate as a model system to study endoplasmic reticulum membrane protein degradation. Methods Mol. Biol. *301*, 185–205.

Carlson, E., Pitonzo, D., and Skach, W. (2006) p97 functions as a non-essential auxiliary factor to facilitate TM-domain extraction during CFTR ER-associated degradation. EMBO J. *25*, 4557–4566.

Cascio, P., Call, M., Petre, B. M., Walz, T., and Goldberg, A. L. (2002). Properties of the hybrid form of the 26S proteasome containing both 19S and PA28 complexes. EMBO J. *21*, 2636–2645.

DeMartino, G. N., and Slaughter, C. A. (1999). The proteasome, a novel protease regulated by multiple mechanisms. J. Biol. Chem. *274*, 22123–22126.

Driscoll, J., and Goldberg, A. L. (1990). The proteasome (multicatalytic protease) is a component of the 1500-kDa proteolytic complex which degrades ubiquitin-conjugated proteins. J. Biol. Chem. *265*, 4789–4792.

Dubiel, W., Ferrell, K., and Rechsteiner, M. (1995). Subunits ofthe regulatory complex of the 26S protease. Mol. Biol. Rep. *21*, 27–34.

Dubiel, W., Pratt, G., Ferrell, K., and Rechsteiner, M. (1992). Purification of an 11 S regulator of the multicatalytic protease. J. Biol. Chem. *267*, 22369–22377.

Eng, J. K., McCormack, A. L., and Yates, J. R., 3rd. (1994). An approach to correlate tandem mass spectral data of peptides with amino acid sequences in a protein database. J. Am. Soc. Mass Spectrom. *5*, 976–989.

Etlinger, J. D., and Goldberg, A. L. (1977). A soluble ATP-dependent proteolytic system responsible for the degradation of abnormal proteins in reticulocytes. Proc. Natl. Acad. Sci. USA *74*, 54–58.

Elsasser, S., Schmidt, M. and Finley, D. Characterization of the proteasome using native gel electrophoresis. Methods Enzymol. *398*, 353–363.

Finley, D., *et al.* (1998). Unified nomenclature for subunits of the *Saccharomyces cerevisiae* proteasome regulatory particle. Trends Biochem. Sci. *23*, 244–245.

Forster, A., Masters, E. I., Whitby, F. G., Robinson, H., and Hill, C. P. (2005). The 1.9 A structure of a proteasome-11S activator complex and implications for proteasome-PAN/PA700 interactions. Mol. Cell *18*, 589–599.

Früh, K., and Yang, Y. (1999). Antigen presentation by MHC class I and its regulation by interferon gamma. Curr. Opin. Immunol. *11*, 76–81.

Glickman, M., and Ciechanover, A. (2002). The ubiquitin-proteasome proteolytic pathway: destruction for the sake of construction. Physiol. Rev. *82*, 373–428.

Glickman, M. H., Rubin, D. M., Fu, H., Larsen, C. N., Coux, O., Wefes, I., Pfeifer, G., Cjeka, Z., Vierstra, R., Baumeister, W., Fried, V., and Finley, D. (1999). Functional analysis of the proteasome regulatory particle. Mol. Biol. Rep. *26*, 21–28.

Gnann, A., Riordan, J., and Wolf, D. (2004). Cystic fibrosis transmembrane conductance regulator degradation depends on the lectins Htmm1p/EDEM and the cdc48 complex in yeast. Mol. Biol. Cell *15*, 4125–4135.

Groll, M., Bajorek, M., Kohler, A., Moroder, L., Rubin, D. M., Huber, R., Glickman, M. H., and Finley, D. (2000). A. gated channel into the proteasome core particle. Nat. Struct. Biol. *7*, 1062–1067.

Groll, M., Ditzel, L., Lowe, J., Stock, D., Bochtler, M., Bartunik, H. D., and Huber, R. (1997). Structure of 20S. proteasome from yeast at 2.4 A. resolution. Nature *386*, 463–471.

Harris, J. L., Alper, P. B., Li, J., Rechsteiner, M., and Backes, B. J. (2001). Substrate specificity of the human proteasome. Chem. Biol. *8*, 1131–1141.

Hendil, K. B., Khan, S., and Tanaka, K. (1998). Simultaneous binding of PA28 and PA700 activators to 20 S proteasomes. Biochem. J. *332*(Pt 3), 749–754.

Hershko, A., Leshinsky, E., Ganoth, D., and Heller, H. (1984). ATP-dependent degradation of ubiquitin-protein conjugates. Proc. Natl. Acad. Sci. USA *81*, 1619–1623.

Hoffman, L., Pratt, G., and Rechsteiner, M. (1992). Multiple forms of the 20 S multicatalytic and the 26 S ubiquitin/ATP-dependent proteases from rabbit reticulocyte lysate. J. Biol. Chem. *267*, 22362–22368.

Keller, A., Nesvizhskii, A. I., Kolker, E., and Aebersold, R. (2002). Empirical statistical model to estimate the accuracy of peptide identifications made by MS/MS and database search. Anal. Chem. *74*, 5383–5392.

Kloetzel, P. M. (2001). Antigen processing by the proteasome. Nat. Rev. Mol. Cell Biol. *2*, 179–187.

Kloetzel, P. M. (2004). The proteasome and MHC class I antigen processing. Biochim. Biophys. Acta *1695*, 225–233.

Kloetzel, P. M., and Ossendorp, F. (2004). Proteasome and peptidase function in MHC-class-I-mediated antigen presentation. Curr. Opin. Immunol. *16*, 76–81.

Kopp, F., Dahlmann, B., and Kuehn, L. (2001). Reconstitution of hybrid proteasomes from purified PA700–20 S complexes and PA28alphabeta activator: ultrastructure and peptidase activities. J. Mol. Biol. *313*, 465–471.

Leggett, D. S., Glickman, M. H., and Finley, D. (2005). Purification of proteasomes, proteasome subcomplexes, and proteasome-associated proteins from budding yeast. Methods Mol. Biol. *301*, 57–70.

Leggett, D. S., Hanna, J., Borodovsky, A., Crosas, B., Schmidt, M., Baker, R., Walz, T., Ploegh, H., and Finley, D. (2002). Multiple associated proteins regulate proteasome structure and function. Cell *10*, 495–507.

Li, J., Gao, X., Ortega, J., Nazif, T., Joss, L., Bogyo, M., Steven, A. C., and Rechsteiner, M. (2001). Lysine 188 substitutions convert the pattern of proteasome activation by REGgamma to that of REGs alpha and beta. EMBO J. *20*, 3359–3369.

Liu, C. W., Strickland, E., Demartino, G. N., and Thomas, P. J. (2005). Recognition and processing of misfolded proteins by PA700, the 19S regulatory complex of the 26S proteasome. Methods Mol. Biol. *301*, 71–81.

Lowe, J., Stock, D., Jap, B., Zwickl, P., Baumeister, W., and Huber, R. (1995). Crystal structure of the 20S proteasome from the archaeon *T. acidophilum* at 3.4 A resolution. Science *268*, 533–539.

Ma, C. P., Slaughter, C. A., and DeMartino, G. N. (1992). Identification, purification, and characterization of a protein activator (PA28) of the 20 S proteasome (macropain). J. Biol. Chem. *267*, 10515–10523.

Mortz, E., Krogh, T. N., Khenrik, V., and Gorg, A. (2001). Improved silver staining protocols compatible with large-scale protein identification using matrix assisted laser desorption/iionization-time of flight analysis. Proteomics *1*, 1359–1363.

Nesvizhskii, A. I., Keller, A., Kolker, E., and Aebersold, R. (2003). A statistical model for identifying proteins by tandem mass spectrometry. Anal. Chem. *75*, 4646–4658.

Oberdorf, J., Carlson, E. J., and Skach, W. R. (2001). Redundancy of mammalian proteasome beta subunit function during endoplasmic reticulum associated degradation. Biochemistry *40*, 13397–13405.

Oberdorf, J., Carlson, E. J., and Skach, W. R. (2006). Uncoupling proteasome peptidase and ATPase activities results in cytosolic release of an ER polytopic protein. J. Cell Sci. *119*, 303–313.

Orino, E., Tanaka, K., Tamura, T., Sone, S., Ogura, T., and Ichihara, A. (1991). ATP-dependent reversible association of proteasomes with multiple protein components to form 26S complexes that degrade ubiquitinated proteins in human HL-60 cells. FEBS Lett. *284*, 206–210.

Pickart, C. M., and Cohen, R. E. (2004). Proteasomes and their kin: proteases inthe machine age. Nat. Rev. Mol. Cell Biol. *5*, 177–187.

Rechsteiner, M., and Hill, C. P. (2005). Mobilizing the proteolytic machine: cell biological roles of proteasome activators and inhibitors. Trends Cell Biol. *15*, 27–33.

Rechsteiner, M., Realini, C., and Ustrell, V. (2000). The proteasome activator 11 SREG (P.A28) and class I antigen presentation. Biochem. J. *345*(Pt 1), 1–15.

Reguenga, C., Oliveira, M. E., Gouveia, A. M., Sa-Miranda, C., and Azevedo, J. E. (2001). Characterization of the mammalian peroxisomal import machinery: Pex2p, Pex5p, Pex12p, and Pex14p are subunits of the same protein assembly. J. Biol. Chem. *276*, 29935–29942.

Rock, K. L., Gramm, C., Rothstein, L., Clark, K., Stein, R., Dick, L., Hwang, D., and Goldberg, A. L. (1994). Inhibitors of the proteasome block the degradation of most cell proteins and the generation of peptides presented on MHC class I molecules. Cell *78*, 761–771.

Saeki, Y., Toh-e, A., and Yokosawa, H. (2000). Rapid isolation and characterization of the yeast proteasome regulatory complex. Biochem. Biophys. Res. Commun. *273*, 509–515.

Schägger, H., Cramer, W. A., and von Jagow, G. (1994). Analysis of molecular masses and oligomeric states of protein complexes by blue native electrophoresis and isolation of membrane protein complexes by two-dimensional native electrophoresis. Anal. Biochem. *217*, 220–230.

Schägger, H., and von Jagow, G. (1991). Blue native electrophoresis for isolation of membrane protein complexes in enzymatically active form. Anal. Biochem. *199*, 223–231.

Shibatani, T., David, L. L., McCormack, A. L., Frueh, K., and Skach, W. R. (2005). Proteomic analysis of mammalian oligosaccharyltransferase reveals multiple subcomplexes that contain Sec61, TRAP, and two potential new subunits. Biochemistry *44*, 5982–5992.

Shibatani, T., and Ward, W. F. (1995). Sodium dodecyl sulfate (SDS) activation of the 20S proteasome in rat liver. Arch. Biochem. Biophys. *321*, 160–166.

Strickland, E., Hakala, K., Thomas, P. J., and DeMartino, G. N. (2000). Recognition of misfolding proteins by PA700, the regulatory subcomplex of the 26 S proteasome. J. Biol. Chem. *275*, 5565–5572.

Tanahashi, N., Murakami, Y., Minami, Y., Shimbara, N., Hendil, K. B., and Tanaka, K. (2000). Hybrid proteasomes. Induction by interferon-gamma and contribution to ATP-dependent proteolysis. J. Biol. Chem. *275*, 14336–14345.

Tanaka, K. (1998). Molecular biology of the proteasome. Biochem. Biophys. Res. Commun. *247*, 537–541.

Tanaka, K., and Tsurumi, C. (1997). The 26S proteasome: subunits and functions. Mol. Biol. Rep. *24*, 3–11.

Tanaka, K., Yoshimura, T., Kumatori, A., Ichihara, A., Ikai, A., Nishigai, M., Kameyama, K., and Takagi, T. (1988). Proteasomes (multi-protease complexes) as 20 S ring-shaped particles in a variety of eukaryotic cells. J. Biol. Chem. *263*, 16209–16217.

Udvardy, A. (1993). Purification and characterization of a multiprotein component of the *Drosophila* 26S (1500 kDa) proteolytic complex. J. Biol. Chem. *268*, 9055–9062.

Verma, R., Chen, S., Feldman, R., Schieltz, D., Yates, J., Dohmen, J., and Deshaies, R. J. (2000). Proteasomal proteomics: identification of nucleotide-sensitive proteasome-interacting proteins by mass spectrometric analysis of affinity-purified proteasomes. Mol. Biol. Cell *11*, 3425–3439.

Voges, D., Zwickl, P., and Baumeister, W. (1999). The 26S proteasome: a molecular machine designed for controlled proteolysis. Annu. Rev. Biochem. *68*, 1015–1068.

Wang, C. C., Bozdech, Z., Liu, C. L., Shipway, A., Backes, B. J., Harris, J. L., and Bogyo, M. (2003). Biochemical analysis of the 20S proteasome of *Trypanosoma brucei*. J. Biol. Chem. *278*, 15800–15808.

Wang, L., and Dobberstein, B. (1999). Oligomeric complexes involved in translocation of proteins across the membrane ofthe endoplasmic reticulum. FEBS Lett. *457*, 316–322.

Wefes, I., Mastrandrea, L. D., Haldeman, M., Koury, S. T., Tamburlin, J., Pickart, C. M., and Finley, D. (1995). Induction of ubiquitin-conjugating enzymes during terminal erythroid differentiation. Proc. Natl. Acad. Sci. USA *92*, 4982–4986.

Whitby, F. G., Masters, E. I., Kramer, L., Knowlton, J. R., Yao, Y., Wang, C. C., and Hill, C. P. (2000). Structural basis for the activation of 20S proteasomes by 11S regulators. Nature *408*, 115–120.

Wittig, I., and Schägger, H. (2005). Advantages and limitations of clear-native PAGE. Proteomics *5*, 4338–4346.

Wolf, D. H., and Hilt, W. (2004). The proteasome: a proteolytic nanomachine of cell regulation and waste disposal. Biochim. Biophys. Acta *1695*, 19–31.

Xiong, X., Chong, E., and Skach, W. R. (1999). Evidence that endoplasmic reticulum (ER)-associated degradation of cystic fibrosis transmembrane conductance regulator is linked to retrograde translocation from the ER membrane. J. Biol. Chem. *274*, 2616–2624.

Yang, Y., Früh, K., Ahn, K., and Peterson, P. A. (1995). In vivo assembly of the proteasomal complexes, implications for antigen processing. J. Biol. Chem. *270*, 27687–27694.

Yoshimura, T., Kameyama, K., Takagi, T., Ikai, A., Tokunaga, F., Koide, T., Tanahashi, N., Tamura, T., Cejka, Z., Baumeister, W., Tanaka, K., and Ichihara, A. (1993). Molecular characterization of the "26S" proteasome complex from rat liver. J. Struct. Biol. *111*, 200–211.